

Clinical Investigation

NRG Oncology Updated International Consensus Atlas on Pelvic Lymph Node Volumes for Intact and Postoperative Prostate Cancer



William A. Hall, MD,* Eric Paulson, PhD,* Brian J. Davis, MD, PhD,[†]
Daniel E. Spratt, MD,[‡] Todd M. Morgan, MD,[§] David Dearnaley, FRCR, MD,^{||}
Alison C. Tree, FRCR, MD,^{||} Jason A. Efstathiou, MD, DPhil, FACRO, FASTRO,[¶]
Mukesh Harisinghani, MD,[#] Ashesh B. Jani, MD, MSEE, FASTRO,**
Mark K. Buyyounouski, MD, MS,^{††} Thomas M. Pisansky, MD,[†]
Phuoc T. Tran, MD, PhD,^{‡‡} R. Jeffrey Karnes, MD,^{§§}
Ronald C. Chen, MD, MPH, FASCO, FASTRO,^{|||} Fabio L. Cury, MD,^{¶¶}
Jeff M. Michalski, MD, MBA, FASTRO,^{##}
Seth A. Rosenthal, MD, FACR, FASTRO,*** Bridget F. Koontz, MD,^{†††}
Anthony C. Wong, MD, PhD,^{‡‡‡} Paul L. Nguyen, MD,^{§§§}
Thomas A. Hope, MD,^{||||} Felix Feng, MD,^{‡‡‡}

Corresponding author: William A. Hall, MD; E-mail: whall@mcw.edu

Disclosures: R.C. reports personal fees from Abbvie and Accuray, outside the submitted work. F.L.C. reports grants and nonfinancial support from Boston Scientific, personal fees from Varian Medical Systems, and grants from Sanofi, outside the submitted work. B.J.D. reports personal fees from Boston Scientific, Inc, outside the submitted work. D.D. reports personal fees from The Institute of Cancer Research, during the conduct of the study; in addition, D.D. has a patent EP1933709B1 issued. J.A.E. reports personal fees from Blue Earth Diagnostics, Boston Scientific, AstraZeneca, Taris Biomedical, Janssen, Bayer Healthcare, and Roivant Pharma, outside the submitted work. F.F. reports personal fees from Dendreon, EMD Serono, Janssen Oncology, Ferring, Sanofi, Bayer, Blue Earth Diagnostics, Celgene, Medivation/Astellas, Clovis Oncology, and Genentech and other from PFS Genomics and Nutcracker Therapeutics, outside the submitted work; in addition, F.F. has a patent EP3047037 A4 issued. W.A.H. reports technical support from MIM Software Inc, during the conduct of the study, and other from Elekta AB, outside the submitted work. T.A.H. reports grants from Philips Healthcare and Advanced Accelerator Applications and personal fees from Curium and Ipsen, outside the submitted work. B.F.K. reports grants from Janssen Scientific Affairs, grants and personal fees from Blue Earth Diagnostics, grants from Merck, and personal fees from Demos Publishing, outside the submitted work. P.L.N. reports personal fees from COTA, Ferring, Astellas, Dendreon, Blue Earth Diagnostics, and Boston Scientific; grants and personal fees from Astellas, Bayer, and Janssen; and personal fees and other from Augmenix, outside the submitted work. E.P. reports other from Elekta AB, outside the submitted work. H.M.S. reports personal fees from Janssen and other from Radiogel, outside the

submitted work and is a member of the ASTRO Board of Directors. D.E.S. reports personal fees from Janssen, Blue Earth, and AstraZeneca, outside the submitted work. P.T.T. reports grants from Astellas Pharm and Bayer Healthcare; grants, personal fees, and other from RefleXion Medical Inc; and personal fees from Noxopharm, outside the submitted work; in addition, P.T.T. has a patent Compounds and Methods of Use in Ablative Radiotherapy (#9114158) licensed to Natsar Pharm. A.C.T. reports grants and personal fees from Elekta; grants from Accuray and Varian; personal fees from Janssen, Genesis healthcare, and Ferring; and nonfinancial support from Astellas, outside the submitted work. All other authors have nothing to disclose.

Data Sharing: Research data are stored in an institutional repository and will be shared upon request to the corresponding author.

Supplementary material for this article can be found at <https://doi.org/10.1016/j.ijrobp.2020.08.034>.

Acknowledgments—Medical College of Wisconsin Libraries and MIM provided technical support (MIM Inc, Beachwood, OH). Katie Kruger provided meeting coordination and manuscript formatting. This work represents independent research supported by the National Institute for Health Research Biomedical Research Centre at The Royal Marsden NHS Foundation Trust and the Institute of Cancer Research, London. The views expressed are those of the authors and not necessarily those of the NIHR or the Department for Health and Social Care. The project described was supported by the National Center for Advancing Translational Sciences, National Institutes of Health, Award Number KL2TR001438. The content is solely the responsibility of the author(s) and does not necessarily represent the official views of the NIH.

Howard M. Sandler, MD, FASCO, FASTRO,^{###} and Colleen A.F. Lawton, MD, FACR, FASTRO^{*}

^{*}Medical College of Wisconsin, Department of Radiation Oncology, Milwaukee, Wisconsin; [†]Mayo Clinic, Department of Radiation Oncology, Rochester, Minnesota; [‡]Department of Radiation Oncology, University of Michigan, Ann Arbor, Michigan; [§]Department of Urology, University of Michigan, Ann Arbor, Michigan; ^{||}The Royal Marsden NHS Foundation Trust and The Institute of Cancer Research, London, UK; [¶]Department of Radiation Oncology, Massachusetts General Hospital, Boston, Massachusetts; [#]Department of Radiology, Massachusetts General Hospital, Boston, Massachusetts; ^{**}Department of Radiation Oncology, Emory University, Atlanta, Georgia; ^{††}Department of Radiation Oncology, Stanford University, Stanford, California; ^{‡‡}Department of Radiation Oncology, Johns Hopkins, Baltimore, Maryland; ^{§§}Department of Urology, Mayo Clinic, Rochester, Minnesota; ^{|||}Department of Radiation Oncology, University of Kansas, Kansas City, Kansas; ^{¶¶}Department of Radiation Oncology, McGill University, Montreal, Canada; ^{##}Department of Radiation Oncology, Washington University, St. Louis, Missouri; ^{***}Department of Radiation Oncology, Sutter Medical Group, Roseville, California; ^{†††}Department of Radiation Oncology, Duke Cancer Institute, Durham, North Carolina; ^{‡‡‡}Department of Radiation Oncology, University of California San Francisco, San Francisco, California; ^{§§§}Department of Radiation Oncology, Dana Farber Harvard Cancer Center, Boston, Massachusetts; ^{||||}Department of Radiology and Biomedical Imaging, University of California San Francisco, San Francisco, California; and ^{###}Department of Radiation Oncology, Cedars-Sinai Medical Center, Los Angeles, California

Received Jun 3, 2020. Accepted for publication Aug 7, 2020.

Purpose: In 2009, the Radiation Therapy Oncology Group (RTOG) genitourinary members published a consensus atlas for contouring prostate pelvic nodal clinical target volumes (CTVs). Data have emerged further informing nodal recurrence patterns. The objective of this study is to provide an updated prostate pelvic nodal consensus atlas.

Methods and Materials: A literature review was performed abstracting data on nodal recurrence patterns. Data were presented to a panel of international experts, including radiation oncologists, radiologists, and urologists. After data review, participants contoured nodal CTVs on 3 cases: postoperative, intact node positive, and intact node negative. Radiation oncologist contours were analyzed qualitatively using count maps, which provided a visual assessment of controversial regions, and quantitatively analyzed using Sorensen-Dice similarity coefficients and Hausdorff distances compared with the 2009 RTOG atlas. Diagnostic radiologists generated a reference table outlining considerations for determining clinical node positivity.

Results: Eighteen radiation oncologists' contours (54 CTVs) were included. Two urologists' volumes were examined in a separate analysis. The mean CTV for the postoperative case was 302 cm³, intact node positive case was 409 cm³, and intact node negative case was 342 cm³. Compared with the original RTOG consensus, the mean Sorensen-Dice similarity coefficient for the postoperative case was 0.63 (standard deviation [SD] 0.13), the intact node positive case was 0.68 (SD 0.13), and the intact node negative case was 0.66 (SD 0.18). The mean Hausdorff distance (in cm) for the postoperative case was 0.24 (SD 0.13), the intact node positive case was 0.23 (SD 0.09), and intact node negative case was 0.33 (SD 0.24). Four regions of CTV controversy were identified, and consensus for each of these areas was reached.

Conclusions: Discordance with the 2009 RTOG consensus atlas was seen in a group of experienced NRG Oncology and international genitourinary radiation oncologists. To address areas of variability and account for new data, an updated NRG Oncology consensus contour atlas was developed. © 2020 Elsevier Inc. All rights reserved.

Introduction

The treatment of pelvic lymph nodes with external beam radiation therapy (RT) is a frequent component of the management of patients with prostate cancer.¹ Pelvic lymph node irradiation is a common practice for men receiving prostate RT with high-risk disease, clinically lymph node-positive disease, and in the postprostatectomy setting.²⁻⁴ There exists a wide range of approaches to pelvic nodal

contouring and identification of pelvic nodal regions considered to be "at risk." Treated volumes also have been historically correlated with clinical outcomes for prostate patients.⁵ The Radiation Therapy Oncology Group (RTOG) developed a consensus-based contouring atlas in 2009 that has served as a foundation for nodal contouring on several prospective clinical trials.⁶ This guideline has also been used in standard clinical practice. A consensus atlas encourages a consistent application of nodal treatments across

providers and institutions to allow additional understanding of the effects of this component of treatment.

Since publication of the original RTOG atlas, additional data on patterns of tumor recurrence have emerged through both retrospective and prospective imaging studies. Multiple publications have presented data to support a change in recommendations for pelvic nodal contouring from the original RTOG consensus atlas.⁷⁻¹¹ Given these data, the NRG Oncology genitourinary (GU) core committee thought it was appropriate to update the consensus atlas for pelvic nodal contouring and to expand the existing atlas to address the postoperative and clinically node-positive settings. The objective of this study was to both expand and refine the existing consensus nodal atlas to account for contemporary research findings.

Methods and Materials

The first and senior authors (W.A.H. and CA.F.L.) along with the NRG Oncology GU core committee recruited an international panel of physicians including radiation oncologists, diagnostic radiologists (with expertise in nuclear medicine and magnetic resonance imaging [MRI]), and urologists. The study was approved by the Institutional Review Board at the Medical College of Wisconsin before initiating research activities. All participants in the contouring effort were informed via e-mail correspondence and verbal review at the start of the video conferencing of their rights as participants in this nodal contouring effort. Care was taken to anonymize individual observer contour contributions within the group.

The first step in the update was a review of the literature on pelvic nodal recurrence patterns published since 2007. This literature search was performed in collaboration with the Medical College of Wisconsin Libraries. Primary search sources included: (1) PubMed (((pelvic AND (lymph node drainage OR lymphatic drainage))) AND prostate cancer) and (2) Google Scholar (terms: prostate cancer nodal drainage, prostate cancer nodal radiation, prostate cancer nodal failure patterns, post-operative prostate cancer nodal failure, prostate-specific membrane antigen [PSMA] nodal failure, fluciclovine F-18 nodal failure patterns, and C-11 Choline PET prostate lymph nodes). Along with the primary search terms, several additional “similar publication” links from the references were used. Finally, all participants were asked to send relevant literature and references to the first author (W.A.H.) for review, organization, and presentation. Publications selected by the group were considered representative of the most recent and relevant data in 4 different categories: (1) existing updated nodal consensus atlases, (2) modern surgical/intact disease lymphatic drainage patterns, (3) postoperative recurrence patterns, and (4) novel molecular positron emission tomography (PET)-based recurrence patterns. Publications were presented in detail via video conference for discussion and commentary from all members in the

group. Figures were reviewed with the group, including locations of failure patterns. Surgeons and radiologists participated in these calls and were available for commentary and questions. After the video conference presentations, slides (with notes from the video conferencing) were circulated to all participants for additional individual review.

After this data presentation, radiation oncologists were asked to contour the nodal CTV. A total of 3 cases formed the primary contouring subjects. These cases were selected by the first and senior authors (W.A.H. and CA.F.L.). Case 1 was a 58-year-old man with a history of unfavorable intermediate-risk adenocarcinoma of the prostate, clinical stage T1cN0M0, grade group 3, Gleason score 4 + 3, and initial serum prostate-specific antigen (PSA) of 5.92 ng/mL, who underwent surgical resection. Final pathology showed grade group 3, Gleason score 4 + 3 adenocarcinoma, positive margins, extensive seminal vesicle involvement, and 1 of 8 nodes positive in a right obturator node (pT3bN1M0). Case 2 was a 66-year-old man with high-risk adenocarcinoma of the prostate who underwent a biopsy due to a PSA rising to 13.7 ng/mL. Biopsy showed grade group 4, Gleason score 4 + 4, with clinical stage of T2bN1M0. He was clinically node positive, with 2 enlarged regional nodes on his diagnostic pelvic computed tomography (CT). Case 3 was a 65-year-old man with high-risk adenocarcinoma of the prostate, clinical stage T2aN0M0, grade group 5, Gleason score 4 + 5, and PSA 38.2 ng/mL.

Urologists (T.M.M. and R.J.K.) were also asked to contour “dissection” regions using their anticipated dissection templates using case 3. These surgical contours were not included in the primary nodal contouring analysis. Contours were completed using MIM cloud (MIM Software Inc, Cleveland, OH). Contouring physician observers were blinded to other participants’ contour results during this process of contouring. Only the first, second, and senior author (W.A.H., EP, and CA.F.L.) had access to all contour results collectively. Observers were required to contour a nodal CTV and, if so inclined, to contour a nodal gross tumor volume.

Contour analysis was performed using the Sorensen-Dice similarity coefficient and Hausdorff distance.^{12,13} These metrics were calculated and compared with a baseline contour that was created by the first (W.A.H.) and senior (CA.F.L.) authors following the 2009 RTOG nodal contouring atlas.⁶ The contour volumes were statistically compared using a Mann-Whitney test. The CTV contours of all individual observers were used to create a count map having the same resolution as the underlying image modality. Within such a count map, each voxel value is determined by the superposition of observers who included the corresponding image voxel within their CTV. For 18 observers, the maximum count is 18. If all image voxels were included in a contour, they would present as a solid single color. If some of the voxels were not included in a contour set, they would present as a different color, based on the number of observers who included those voxels.

Within a count map, different iso-surfaces with different colors were created. A total of 18 colors would be available with 18 observers. This enabled very careful “qualitative” observation of specific regions that were controversial and presented a method to highlight specific areas of controversy for focused discussion and arbitration. The spread in volume over these percentile surfaces provided an indication of the CTV similarities within the observers and highlighted controversial regions. This method also provided a means by which to visually highlight particular areas of disagreement that were present in contoured volumes among the observers. Diagnostic radiologists (T.A.H. and M.H.) presented a summary of criteria for node positivity in the pelvis using a variety of imaging modalities (Fig. 1).

Results of the consensus contouring exercise were subsequently reviewed at the January 2020 NRG Oncology meeting in person for those attending and were simultaneously presented via video conference for those unavailable to attend. Finally, areas of controversy identified in the contour analytics were adjudicated via an anonymous online survey. The new step-by-step contour recommendations were reviewed and circulated to the group. Common dose and fractionation schedules and corresponding constraints were included for group review and comment. Community radiation oncology feedback on these updates was solicited from the Michigan Radiation Oncology Quality Consortium via video conference and e-mail.

Results

Eighteen radiation oncologists finished 3 full contour sets for a total of 54 volumes, all of which were included in the final contour analysis. The urologists’ contours were not included in the final consensus contour analysis but instead were used for observation and consideration only. Observers practiced in the United States, Canada, and the United Kingdom with a median of more than 15 years of practice.

The mean CTV for the postoperative case was 302 cm³, the intact node positive case was 409 cm³, and the intact node negative case was 342 cm³. Compared with the original RTOG consensus atlas contour (created by authors W.A.H. and C.A.F.L.), the mean Sorensen-Dice similarity coefficient for the postoperative case was 0.63 (SD 0.13), the intact node positive case was 0.68 (SD 0.13), and the intact node negative case was 0.66 (SD 0.18). The mean Hausdorff distance (in centimeters) for the postoperative case was 0.24 (SD 0.13), the intact node positive case was 0.23 (SD 0.09), and the intact node negative case was 0.33 (SD 0.24). These values represented the “quantitative” contour results.

Several “qualitative” variations were identified when using the count maps. Taken collectively, these variations provided a visual representation of consensus (“warmer” colors, e.g., yellow, green) and controversial (“cooler” colors, e.g., magenta) areas. The 4 areas of greatest variability consisted of (1) the superior-most aspect of the common iliac nodes, (2) the transition from the external

| Anatomic Location | CT/MRI-based Size | CT/MRI-based Morphology | PSMA PET-based Criteria | Fluciclovine PET-based Criteria | Example of positive node on CT | Example of positive node on MR | Example of positive node on PET |
|---------------------------------|-------------------|----------------------------------------------------------------------------|----------------------------------------------|--------------------------------------------------------------------------|--------------------------------|--------------------------------|---------------------------------|
| Mesorectal, Presacral | Short axis > 4 mm | Irregular Border and/or heterogenous morphology (only for LN > 3mm on MRI) | Uptake greater than blood pool | > 1 cm: Uptake greater than BM < 1 cm: Uptake greater than blood pool | | | |
| Internal Iliac, Obturator | Short axis > 7mm | Irregular Border and/or heterogenous morphology | Uptake greater than blood pool | > 1 cm: Uptake greater than BM < 1 cm: Uptake greater than blood pool | | | |
| Common Iliac and External Iliac | Short axis > 8 mm | Irregular Border and/or heterogenous morphology | Uptake greater than blood pool | > 1 cm: Uptake greater than BM < 1 cm: Uptake greater than blood pool | | | |
| Inguinal | Short axis > 8 mm | Irregular Border and/or heterogenous morphology | Asymmetric uptake that is greater than liver | Asymmetric uptake greater than BM | | | |

Fig. 1. Summary criteria for clinical node positivity. *Abbreviations:* CT = computed tomography; LN = lymph node; MRI = magnetic resonance imaging; PET = positron emission tomography; PSMA = prostate-specific membrane antigen.

iliac to the inguinal nodes, (3) the inclusion of the periprostatic nodes, and (4) the inclusion of perirectal nodes (Fig. 2a-d). Contours of clinically positive nodes were also controversial. These areas were discussed in detail via an in-person meeting and a video conference and were the subject of specific questions in the anonymous survey. The results of the survey formed the consensus steps (1-10). Consensus on final borders for each of these areas was reached via a written survey specifically addressing potential changes to these areas. The refined steps to contour the nodal CTV can be seen in Figures 3 and 4.

Prophylactic nodal contouring steps for clinically node-negative patients including both intact and postoperative cases (Fig. 3a-m and Fig. 4a-g):

1. Commence contours at the bifurcation of the aorta into the common iliac arteries or the proximal inferior vena cava to the common iliac veins, whichever occurs more superiorly (typically at the level of L4-L5; Fig. 3a-b).
2. Contour approximately 5 to 7 mm around each iliac vessel, including the entire circumference of both the iliac artery and vein. Bone, bowel, bladder, and muscle should be excluded from the nodal CTV contour. Where clinically indicated, CTV margins can be more generous, particularly anterior to vessels (10 mm). Ensure coverage posteriorly in the area formed between the psoas major and the vertebral body (Fig. 3c-d).
3. The width of the interspace between the external and internal iliac contours should be approximately 1.5 to 3 cm. This will vary depending on patient anatomy (Fig. 3e).
4. Include the prevertebral, presacral, and posterior mesorectal nodes to the bottom of S3 (Fig. 3f).
5. The posterior border of the CTV coming off the internal iliac vessels should extend to the anterior edge of the piriformis muscle after the course of the pudendal artery and inferior gluteal artery (Fig. 3g-h).
6. The transition from the external iliac to the inguinal nodes occurs when the external iliac vessels cross beneath the inguinal ligament into the inguinal canal. Examine for this transition and begin tapering off external iliac nodes at that point. This should correspond to the entrance of the

vascular structures into the inguinal canal (Fig. 3i), often best seen on the coronal images (Fig. 3j).

7. The external iliac contours should typically end when the vessels are completely lateral to the most medial aspect of the acetabulum (near the mid-femoral head and fovea). At that point, the contours should be tapered off (Fig. 3k-l).
8. The obturator nodes can be between 1 and 2 cm in width and should extend to the posterior edge of the obturator internus muscle (Fig. 3k).
9. Begin to taper the obturator nodes at the top of the seminal vesicles (or the top of the postoperative bed), extending approximately 1 cm anterior to the anterior edge of the obturator internus muscle (Fig. 3k-l; MRI registration can be useful in this area).
10. The obturator nodes should end where the seminal vesicles join the prostate, or approximately the midportion of the contoured postoperative CTV bed (Fig. 3m).

Modifications when treating clinically node positive cases:

1. Steps 1 to 10 should be followed for prophylactic regions.
2. Figure 1 should be referenced to help identify suspicious nodes; all suspicious nodes should be considered for review with diagnostic radiology and contoured as appropriate.
3. Prophylactic nodal volumes should extend approximately 5 to 7 mm around clinically suspicious nodes; this may alter the prophylactic nodal volumes in steps 1 to 10.
4. Residual (shrunk) gross nodes, post-androgen deprivation therapy (ADT), should form the primary boost volume (additional information in dosing section below).

Radiation dosing to pelvic nodes:

- Prophylactic nodes: A dose range of 45 to 50.4 Gy is acceptable when using conventional fractionation. The majority of participants do not change their prophylactic nodal dose whether treating an intact prostate case or postoperative.

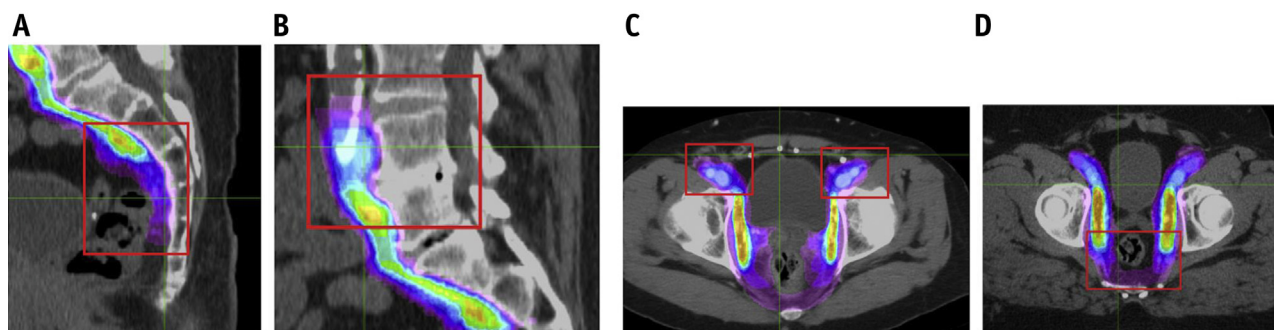


Fig. 2. Count maps showing controversial regions identified.

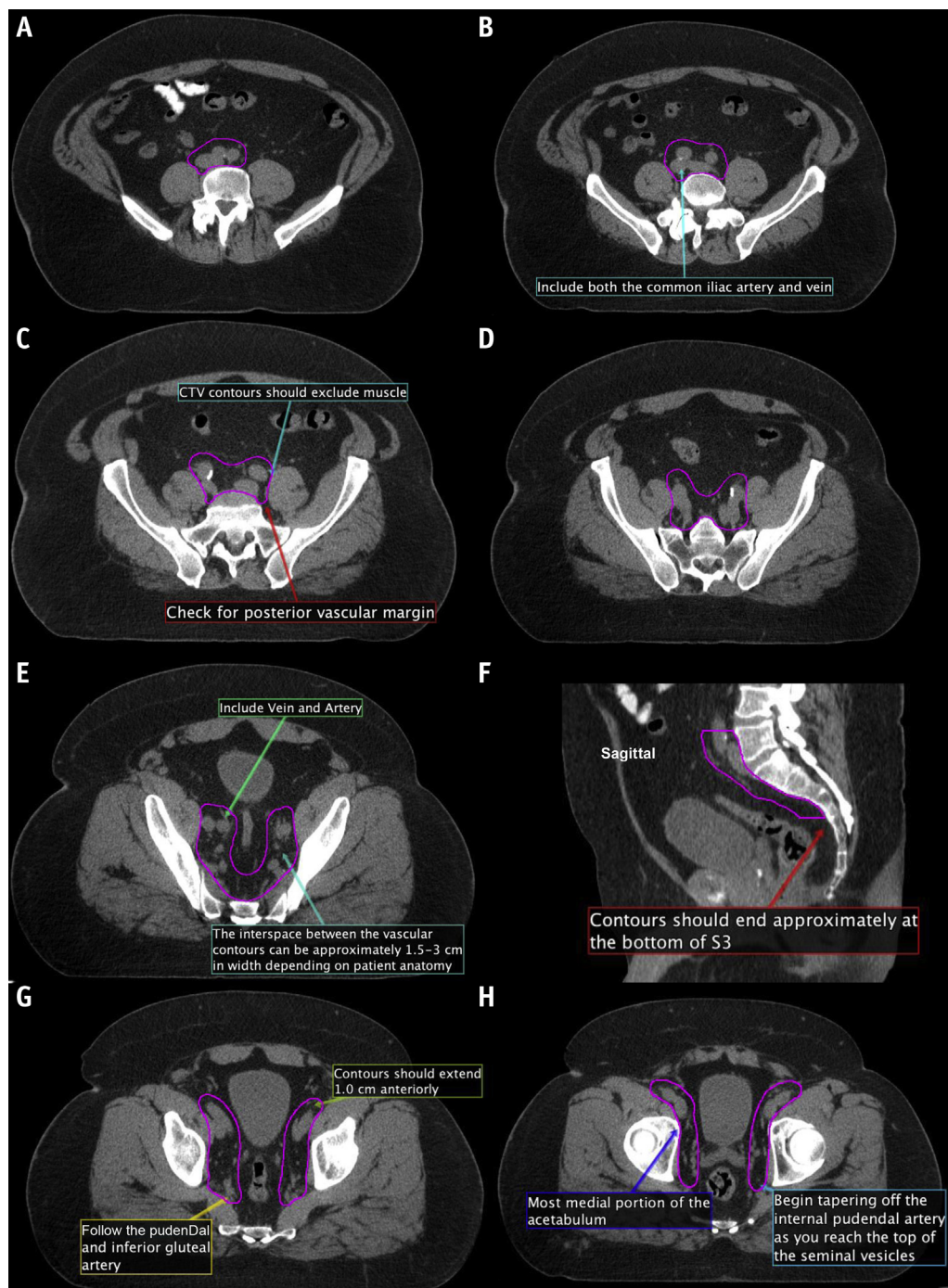


Fig. 3. (A-M) New consensus contours on computed tomography. *Abbreviation:* CTV = clinical target volumes.

- Gross nodes: Should be treated as high as clinically feasible (up to the dose being delivered to the primary tumor) while respecting normal organ tolerances. Nodal volumes should be examined pre- and post-ADT, and the post-ADT tumor volume should serve as the high dose boost volume.

Overarching points for consideration when contouring pelvic nodes with the new guidelines:

- All available/relevant scans (eg, PET and MRI) should be carefully considered by the radiation oncologist when delineating nodal coverage.
- In general, the CTV should exclude bone, bladder, muscle, and bowel.
- Simulation images that are suggestive of clinically suspicious nodes (criteria in Fig. 1) should be reviewed with a

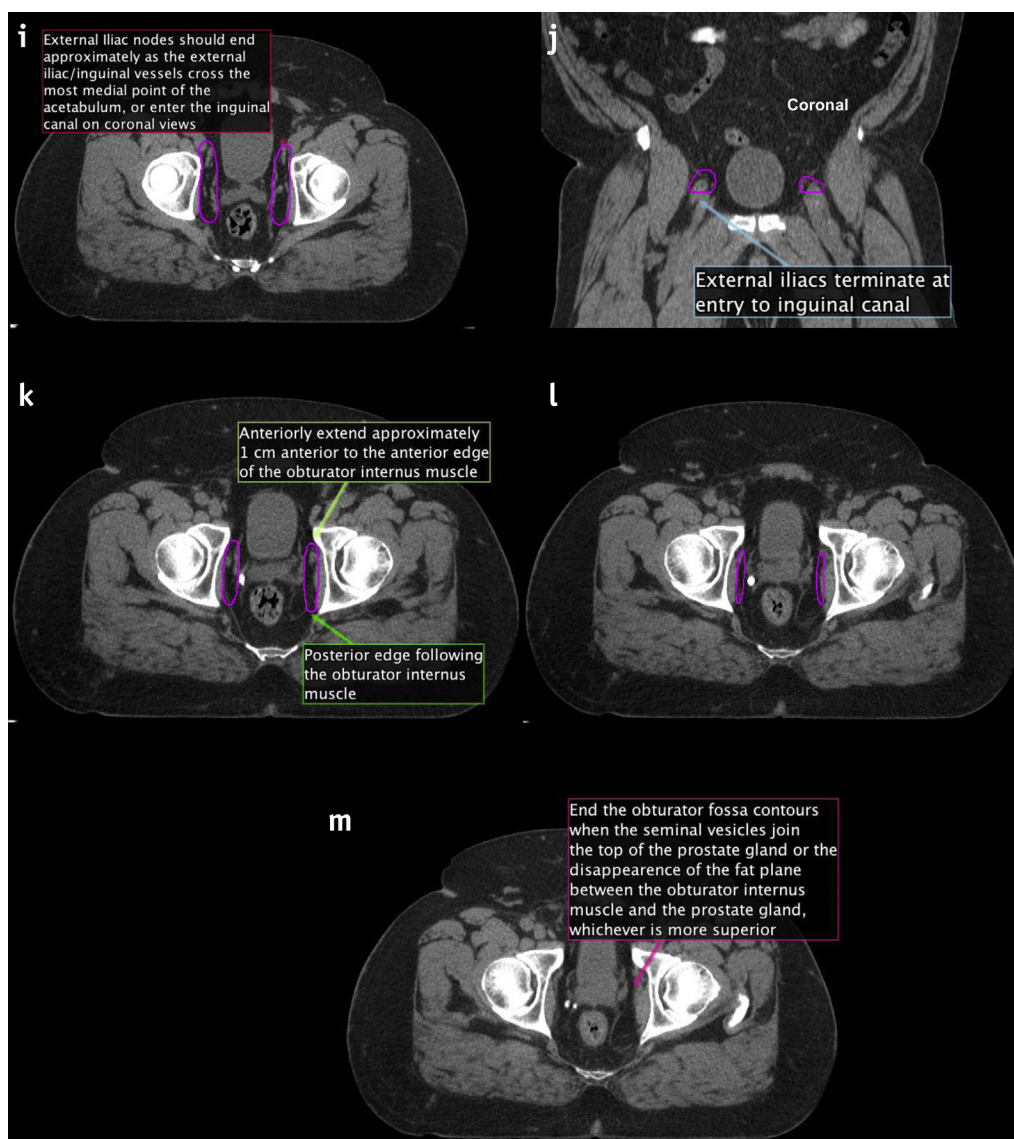


Fig. 3. (continued).

diagnostic radiologist and may be included in boost volumes at the clinical discretion of the radiation oncologist.

- In some circumstances, small portions of bowel may abut vascular structures or large portions of small bowel may be in the pelvis. As mentioned earlier (in step 2), the CTV should exclude bowel (including both small and large bowel). Rarely, bowel may be included in the CTV at the discretion of the radiation oncologist secondary to extenuating clinical circumstances (eg, adjacent involved node or tumor extension). Normal tissue constraints should be prioritized by the radiation oncologist when treating pelvic nodes. Clinical review and discretion on the part of the radiation oncologist is needed in each of these circumstances.
- For postoperative cases: Pathology and operative reports should be carefully considered in treatment volumes. Regions with pathologically involved nodes that

exhibit extranodal tumor extension may have more generous CTVs. Surgical clips should be identified and potentially included at the discretion of the radiation oncologist. Close collaboration with colleagues having expertise in urology and diagnostic radiology is recommended. Altered lymph node spread is common,¹⁴ and larger volume expansions, including postoperative changes of uncertain significance, may also be necessary. PET scans or other advanced imaging acquired should be registered and included in the treatment planning process.

- Consideration should be given to the comorbidities and medical history of each individual patient.

The results of areas that urologic surgeons identified as part of their dissection template are presented in [Figure E1](#). Finally, given the wide range of contour volumes, an example of a larger contour set, including perirectal nodes,

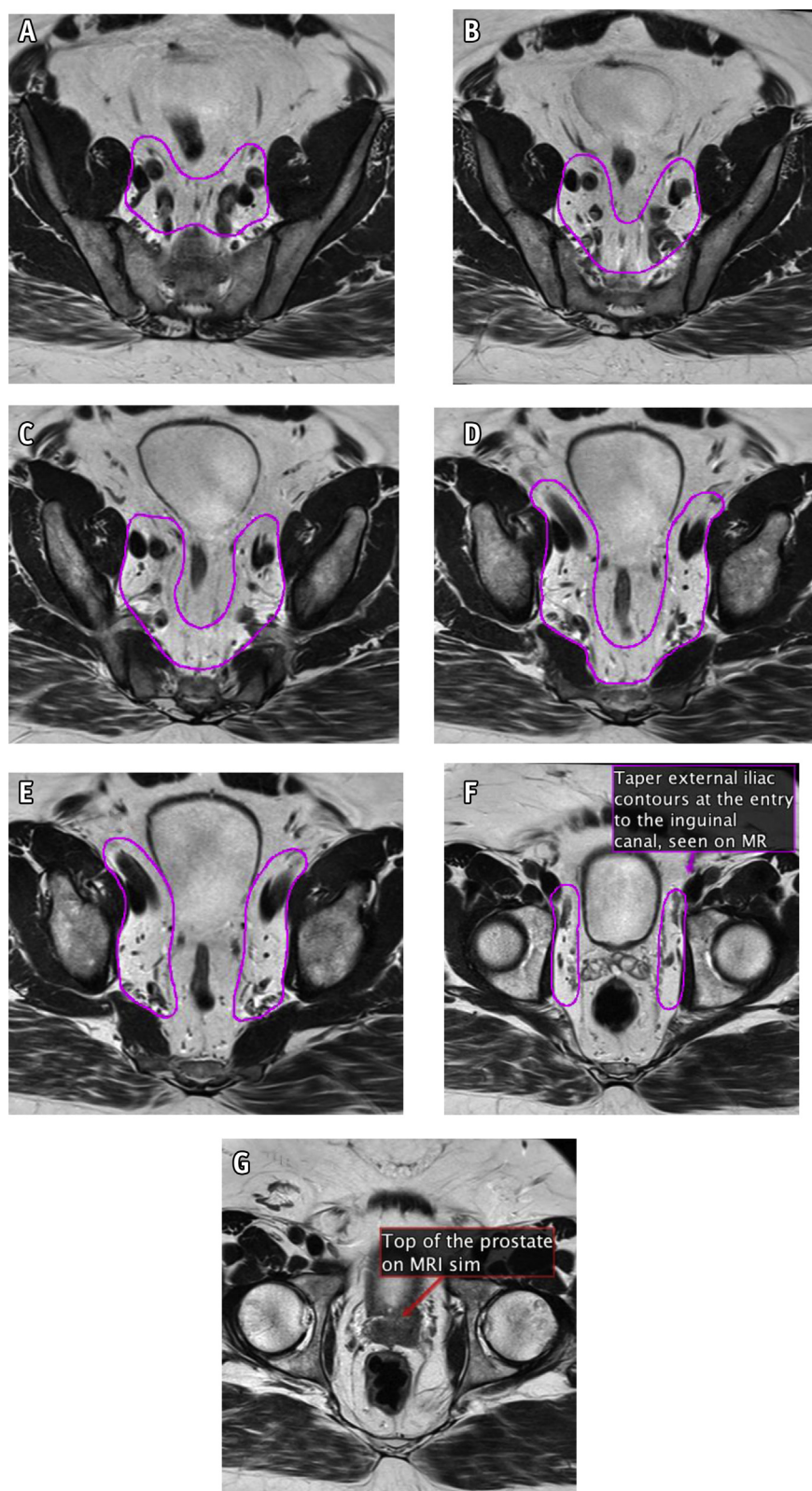


Fig. 4. (A-G): New consensus contours on magnetic resonance.

Table 1 Constraints for consideration when treating pelvic nodes

| 75.6-79.2 Gy in 42-44 fractions, treating nodes to 45-50.4 Gy with a sequential boost | |
|------------------------------------------------------------------------------------------------|----------------------------------------------------------------------------------------------------------------------------------------------------------------------------------------------------------------|
| Rectum (24) | V (≥ 4500 cGy) $\leq 50\%$ V (≥ 7000 cGy) $\leq 15\%$ V (> 7200 cGy) < 10 cm ³ |
| Bladder | V (≥ 4500 cGy) $\leq 50\%$ V (≥ 7000 cGy) $\leq 15\%$ |
| Femur_L | V (≥ 5000 cGy) $\leq 2\%$ Dmax ≤ 5250 cGy |
| Femur_R | V (≥ 5000 cGy) $\leq 2\%$ Dmax ≤ 5250 cGy |
| Colon | V (≥ 6000 cGy) $\leq 2\%$ Dmax ≤ 6250 cGy |
| Small bowel (bowel loops) | V (≥ 5000 cGy) $\leq 10\%$ Dmax ≤ 5200 cGy |
| Pubic bone | V (≥ 7000 cGy) $\leq 25\%$ |
| Penile bulb (should not sacrifice PTV coverage) | V (≥ 5000 cGy) $\leq 50\%$ |
| 70 Gy in 28 fractions, treating nodes to 45-50.4 Gy with a simultaneous integrated boost | |
| Rectum (24) | V (≥ 4500 cGy) $\leq 45\%$ V (≥ 5500 cGy) $\leq 25\%$ V (≥ 6500 cGy) $\leq 15\%$ V (> 6500 cGy) < 10 cm ³ |
| Bladder | V (≥ 4500 cGy) $\leq 45\%$ V (≥ 5500 cGy) $\leq 25\%$ V (≥ 6500 cGy) $\leq 15\%$ |
| Femur_L | V (≥ 5000 cGy) $\leq 1\%$ Dmax ≤ 5250 cGy |
| Femur_R | V (≥ 5000 cGy) $\leq 1\%$ Dmax ≤ 5250 cGy |
| Colon | Dmax ≤ 5500 cGy |
| Small bowel (bowel loops) | V (≥ 4650 cGy) ≤ 2 cm ³ Dmax ≤ 5200 cGy |
| Pubic bone | V (≥ 6000 cGy) $\leq 30\%$ |
| Penile bulb (should not sacrifice PTV coverage) | Make dose as low as reasonably achievable |
| 60 Gy in 20 fractions (treating nodes to 44-47 Gy over 20 fractions*) (8) | |
| Rectum (22) | V (≥ 2000 cGy) $\leq 85\%$ (no circumferential dose) V (≥ 3000 cGy) $\leq 57\%$ V (≥ 4000 cGy) $\leq 38\%$ V (≥ 5000 cGy) $\leq 22\%$ V (≥ 6000 cGy) $\leq 1\%$ † |
| Bladder‡ | V (≥ 4000 cGy) $\leq 50\%$ V (≥ 4800 cGy) $\leq 25\%$ V (≥ 5680 cGy) $\leq 5\%$ V (≥ 6000 cGy) $\leq 3\%$ |
| Femur_L | V (≥ 3500 cGy) $\leq 5\%$ Dmax ≤ 3700 cGy |

(continued)

Table 1 (continued)

| 60 Gy in 20 fractions (treating nodes to 44-47 Gy over 20 fractions*) (8) | |
|---------------------------------------------------------------------------------|---------------------------------------------------------------------------------------------------------------------------|
| Femur_R | V (≥ 3500 cGy) $\leq 5\%$ Dmax ≤ 3700 cGy |
| Colon | Dmax ≤ 5000 cGy |
| Small bowel (bowel loops) | Dmax ≤ 4000 cGy V (≥ 3700 cGy) ≤ 90 cm ³ V (≥ 3300 cGy) ≤ 130 cm ³ |
| Pubic bone | V (≥ 5700 cGy) $\leq 20\%$ |
| Penile bulb (25) | V (≥ 2200 cGy) $\leq 50\%$ |

Abbreviation: PTV = planning target volume.

* Safety and efficacy of hypofractionation to pelvic nodes is currently the subject of ongoing investigation and has not been established.

† Group consensus constraint.

‡ Patient reported quality of life data for the bladder constraints is the subject of ongoing investigation.

can be seen in Figure E2. Such expanded volumes may be rarely considered for highly select and advanced T4 lesions at the discretion of the radiation oncologist.¹⁵ Considerable discretion is needed when including mesorectal nodes in the treatment volume, and normal tissue constraints should be prioritized.

Figure 1 was created by the diagnostic radiologists (T.A.H., M.H.) and nuclear medicine expert (T.A.H.) to include criteria for clinical node positive prostate lesions.¹⁶⁻²¹ These criteria are helpful for radiation oncologists to be aware of and most importantly discuss with their diagnostic radiology and nuclear medicine colleagues. In addition, commonly used dose constraints were collated for different dose and fractionation schedules and are displayed in Table 1.²²⁻²⁵ These may be helpful for radiation oncologists to consider when treating pelvic nodes.

Discussion

Prophylactic treatment of pelvic lymph nodes in the management of prostate cancer remains an active area of clinical inquiry and investigation that presently lacks consensus. Data are emerging suggesting some efficacy to pelvic nodal treatment.¹ In the context of this ongoing inquiry, expert consensus-based guidelines consider its use an acceptable management option.^{3,4} Constant evaluation and evidence-based updating of available consensus guidelines are imperative. Careful examination of the evolution of guidelines over time is essential to ensure evidence-based improvement. The overarching goal of our process was to perform a timely evaluation and update the 2009 RTOG consensus guidelines. We did not seek to reinvent the atlas, but rather sought to update and refine it.

Our study shows the 2009 RTOG pelvic lymph node consensus guidelines no longer accurately reflect the practice patterns of prostate cancer experts from around the world or the state-of-the-art assessment of lymph node regions at risk for prostate cancer metastasis. Furthermore, we developed a guideline process to develop treatment volume contouring standards that could be used as a template for other disease sites, and for research or clinical collaboratives.

These guidelines were updated using an evidence-based process. Several categories of updated data were considered in detail by the group of observers who participated in this contouring effort. These publications fell into 4 broad categories: (1) existing updates to contouring guidelines, (2) surgical mapping and lymphatic drainage series, (3) clinical recurrence series, and (4) PET/postoperative recurrence series. International groups have proposed a few modifications to the existing RTOG nodal contouring atlas that were considered in detail by the authors. The first was an updated atlas produced by the PIVOTAL trialists group,⁸ of which one author (D.D.) also participated as an international representative in this NRG Oncology contouring activity. The PIVOTAL atlas recommended modifications to the existing RTOG contouring recommendations but did not include node-positive, PET, MRI, or postoperative nodal contouring recommendations. The second recently updated consensus atlas that specifically focused on prostate nodal treatment was from the Groupe d'Etude des Tumeurs Uro-Génitales.⁷ This atlas incorporated some novel PET recurrence pattern data available at that time. The Groupe d'Etude des Tumeurs Uro-Génitales atlas does not include specific contouring recommendations for node-positive or postoperative patients. The NRG Oncology group provides the current updated consensus atlas with 3 overarching goals: (1) refining the current RTOG intact prophylactic atlas recommendations, (2) addressing clinically node-positive disease, and (3) addressing contouring in the postoperative setting.

The second broad category of data considered was newly available surgical data. Much of this focused on novel sentinel node data and other surgical nodal mapping techniques. Current surgical methods of addressing pelvic nodes were considered. Most contemporary surgical guidelines recommend an extended pelvic lymph node dissection when a nodal dissection is performed.^{4,26,27} Surgical dissection and nodal mapping data provided valuable insight into common sites of nodal drainage. These data partially informed the updated nodal atlas recommendations. It is notable that the internal iliac, external iliac, and obturator nodes comprise the vast majority of nodal drainage sites of the prostate. However, the common iliac, presacral, and paraortic/caval nodes can also represent 10% or more of nodal drainage sites mapped.^{26,28-31} Other drainage sites, such as perirectal nodes, have also represented more than 10% of nodal drainage sites in some sentinel node mapping series, but this is highly variable and inconsistent.³¹ Appropriate applications of the data were

considered carefully by the panel; it should be noted that inclusion of these more generous nodal volumes should be highly selected.

The third general category of data considered included novel MRI techniques and newly published clinical patterns of recurrence data. Several series directly compared the anatomic distribution of nodal metastases with the published RTOG contouring guideline. Meijer et al examined magnetic resonance lymphography in a modern cohort of intact intermediate- and high-risk patients and noted that more than 50% of patients had positive nodes outside of the RTOG nodal atlas—contoured volumes. Common sites were in the high common iliac, perirectal, and paraortic regions.⁹ It was also noted that a high percentage of patients in the postoperative setting had aberrant nodal spread, with a particularly large percentage of patients exhibiting nodal spread in the perirectal area.¹⁴ Data on patterns of recurrence have also been published directly comparing failure patterns to the existing RTOG atlas. Spratt et al conducted a retrospective series of pelvic nodal failures and mapped those in relation to the existing RTOG nodal atlas.¹⁰ This series concluded that an increase in the superior border of the pelvic nodal treatment volume to cover the common iliac stations to L4/L5 would cover more than 90% of first nodal recurrences.¹⁰ Such findings regarding the common iliac nodal stations have been supported by other publications, demonstrating that a number of recurrences were located outside of the standard RTOG atlas treatment volumes.^{32,33}

The final category of contemporary data considered was novel prostate-specific PET data. More specifically, how prostate PET scans might influence nodal volumes in both the intact treatment naïve setting and the postoperative, biochemically recurrent setting. Series including PSMA, Fluciclovine F18, and C-11 choline PET were considered and reviewed. Several of the published PSMA PET series mapped areas of nodal recurrence that were outside of the existing RTOG template. These recurrence locations were presented and reviewed by the observers for consideration as to how this might influence the existing nodal treatment volumes.^{11,34-38} Several of these series visually mapped PET recurrence locations in relation to the existing RTOG consensus atlas.³⁹

After the literature review, a comprehensive contouring exercise took place. There were both quantitative and qualitative assessments of these contour results. The quantitative results of the contouring exercise yielded Sorensen-Dice coefficients reflecting poor agreement.⁴⁰ These findings were consistent within the postoperative contours, intact node positive, and intact node negative contour sets. Qualitatively, a total of 4 areas were visually identified as controversial using the count map strategy. The count map strategy was believed to be very helpful to recognize areas needing focused discussion as compared with just the numerical metrics. Considered collectively, these metrics were supportive of the need for an updated consensus contouring atlas. Several areas of this updated

atlas differ from the existing 2009 RTOG atlas, including the superior, vascular margins, and inferior boundary recommendations.

A few important points must be considered when examining the new contouring steps presented. These are intended to provide approximate guidelines, not to rigidly constrain the radiation oncologist from exercising clinical judgment in an individual case. Radiation oncologists should carefully examine and incorporate all oncologic and diagnostic scan information into their treatment plans. Some clinical circumstances may warrant more generous treatment volumes or more constrained treatment volumes. Factors specific to the comorbidities and individual patient's medical history should also be considered. We have presented variations for consideration, along with step-by-step guidelines to ensure an overarching consensus recommendation.

As novel PET-based imaging continues to develop, this additional information may help individualize RT planning. Many published series highlight apparently atypical anatomic sites of nodal recurrence, such as in perirectal or periaortic nodes.³⁹ Perirectal nodes in particular were a source of significant discussion, especially for T4 tumors.¹⁵ Routinely including areas such as the perirectal region was thought by the majority of the group to create an unnecessarily large treatment volume. However, a variation in contours is also presented for consideration (Fig. E2) when considered clinically indicated by the radiation oncologist. Other studies have recently addressed considerably more generous treatment volumes and the tolerance of such an approach.⁴¹ As mentioned, advanced molecular imaging studies should be reviewed by radiation oncologists, in collaboration with nuclear medicine, whenever available.

There are limitations to this activity that merit consideration. We do not address the controversial topic of “indications” for pelvic nodal RT. That is currently the subject of multiple trials (NCT01368588, NCT01952223, ISRCTN80146950) and is considered beyond the scope of the present study. This study does not aggregate or meta-analyze formally all reported PET-based patterns of failure; this was also considered beyond the scope of the present study. We also did not address the ideal planning target volume definition. This will depend on target proximity to organs at risk and image guidance methods. This is a consensus atlas that went through extensive revision, refinement, and peer review, but prospective validation of the atlas was not formally conducted. Dosimetric constraints are presented for consideration; however, optimal dose constraints were not the primary focus of the analysis, and these should be interpreted accordingly. Finally, we acknowledge that any guideline is a work in progress and that refinement and enhancement is expected as the science that forms its basis advances.

The objective and results of this study serve as a refinement and evidence-based update to the existing RTOG atlas. Our aspiration was to account for recently

published PET- and MRI-based nodal recurrence data, which support a prudent expansion of target volumes. In addition, we have presented higher resolution CT and MRI sets, with annotations that may assist in educating and obtaining uniformity of practice. Full DICOM image files, with contoured structure sets, are available as supplements to provide greater detail for practitioners.

Conclusions

A new NRG Oncology consensus nodal contouring atlas is presented, with several changes to the existing RTOG consensus atlas. Extensive imaging data and studies provided a basis for the CTVs that radiation oncologists should consider when targeting pelvic nodal tissues. The included guidelines are intended to provide greater detail and account for recently published nodal failure pattern data. Moreover, variations in contouring strategies are presented, along with dosimetric constraints for consideration when treating the pelvic lymph nodes.

References

1. Pollack A, Karrison T, Balogh JA, Low D, Bruner D. Short term androgen deprivation therapy without or with pelvic lymph node treatment added to prostate bed only salvage radiotherapy: The NRG Oncology/RTOG 0534 SPPORT trial. *Int J Radiat Oncol Biol Phys* 2018;102:1605.
2. Lieng H, Kneebone A, Hayden AJ, et al. Radiotherapy for node-positive prostate cancer: 2019 recommendations of the Australian and New Zealand Radiation Oncology Genito-Urinary group. *Radiother Oncol* 2019;140:68-75.
3. Heidenreich A, Bastian PJ, Bellmunt J, et al. EAU guidelines on prostate cancer. Part 1: screening, diagnosis, and local treatment with curative intent-update 2013. *Eur Urol* 2014;65:124-137.
4. Mohler JL, Antonarakis ES, Armstrong AJ, et al. Prostate cancer, version 2.2019, NCCN clinical practice guidelines in oncology. *J Natl Compr Canc Netw* 2019;17:479-505.
5. Roach M 3rd, DeSilvio M, Valicenti R, et al. Whole-pelvis, “mini-pelvis,” or prostate-only external beam radiotherapy after neoadjuvant and concurrent hormonal therapy in patients treated in the Radiation Therapy Oncology Group 9413 trial. *Int J Radiat Oncol Biol Phys* 2006;66:647-653.
6. Lawton CA, Michalski J, El-Naqa I, et al. RTOG GU Radiation oncology specialists reach consensus on pelvic lymph node volumes for high-risk prostate cancer. *Int J Radiat Oncol Biol Phys* 2009;74:383-387.
7. Sargos P, Guerif S, Latorzeff I, et al. Definition of lymph node areas for radiotherapy of prostate cancer: A critical literature review by the French Genito-Urinary Group and the French Association of Urology (GETUG-AFU). *Cancer Treat Rev* 2015;41:814-820.
8. Harris VA, Staffurth J, Naismith O, et al. Consensus guidelines and contouring atlas for pelvic node delineation in prostate and pelvic node intensity modulated radiation therapy. *Int J Radiat Oncol Biol Phys* 2015;92:874-883.
9. Meijer HJ, Fortuin AS, van Lin EN, et al. Geographical distribution of lymph node metastases on MR lymphography in prostate cancer patients. *Radiother Oncol* 2013;106:59-63.
10. Spratt DE, Vargas HA, Zumsteg ZS, et al. Patterns of lymph node failure after dose-escalated radiotherapy: Implications for extended pelvic lymph node coverage. *Eur Urol* 2017;71:37-43.

11. Schiller K, Devecka M, Maurer T, et al. Impact of ^{68}Ga -PSMA-PET imaging on target volume definition and guidelines in radiation oncology: Patterns of failure analysis in patients with primary diagnosis of prostate cancer. *Radiat Oncol* 2018;13:36.
12. Taha AA, Hanbury A. An efficient algorithm for calculating the exact Hausdorff distance. *IEEE Trans Pattern Anal Mach Intell* 2015;37:2153-2163.
13. Sorensen-Dice. MathWorks. Available at: <https://www.mathworks.com/help/images/ref/dice.html>. Accessed January, 3, 2020.
14. Meijer HJ, van Lin EN, Debats OA, et al. High occurrence of aberrant lymph node spread on magnetic resonance lymphography in prostate cancer patients with a biochemical recurrence after radical prostatectomy. *Int J Radiat Oncol Biol Phys* 2012;82:1405-1410.
15. Abu-Gheida I, Bathala TK, Maldonado JA, et al. Increased frequency of mesorectal and perirectal LN involvement in T4 prostate cancers. *Int J Radiat Oncol Biol Phys* 2020.
16. Ramirez M, Ingrand P, Richer JP, et al. What is the pelvic lymph node normal size? Determination from normal MRI examinations. *Surg Radiol Anat* 2016;38:425-431.
17. Maurer T, Eiber M, Schwaiger M, Gschwend JE. Current use of PSMA-PET in prostate cancer management. *Nat Rev Urol* 2016;13:226-235.
18. Hofman MS, Lawrentschuk N, Francis RJ, et al. Prostate-specific membrane antigen PET-CT in patients with high-risk prostate cancer before curative-intent surgery or radiotherapy (proPSMA): A prospective, randomised, multi-centre study. *Lancet* 2020;395.
19. Songmen S, Nepal P, Olsavsky T, Sapire J. Axumin positron emission tomography: Novel agent for prostate cancer biochemical recurrence. *J Clin Imaging Sci* 2019;9:49.
20. Eiber M, Herrmann K, Calais J, et al. Prostate Cancer Molecular Imaging Standardized Evaluation (PROMISE): Proposed mTNM classification for the interpretation of PSMA-ligand PET/CT. *J Nucl Med* 2018;59:469-478.
21. Savir-Baruch B, Banks KP, McConathy JE, et al. ACR-ACNM practice parameter for the performance of fluorine-18 fluciclovine-PET/CT for recurrent prostate cancer. *Clin Nucl Med* 2018;43:909-917.
22. Wilkins A, Naismith O, Brand D, et al. Derivation of dose/volume constraints for the anorectum from clinician- and patient-reported outcomes in the CHHiP trial of radiation therapy fractionation. *Int J Radiat Oncol Biol Phys* 2020;106:928-938.
23. Ferreira MR, Thomas K, Truelove L, et al. Dosimetry and gastrointestinal toxicity relationships in a phase II trial of pelvic lymph node radiotherapy in advanced localised prostate cancer. *Clin Oncol (R Coll Radiol)* 2019;31:374-384.
24. Michalski JM, Gay H, Jackson A, Tucker SL, Deasy JO. Radiation dose-volume effects in radiation-induced rectal injury. *Int J Radiat Oncol Biol Phys* 2010;76(3 Suppl):S123-S129.
25. Murray J, Gulliford S, Griffin C, et al. Evaluation of erectile potency and radiation dose to the penile bulb using image guided radiotherapy in the CHHiP trial. *Clin Transl Radiat Oncol* 2020;21:77-84.
26. Mattei A, Fuechsel FG, Bhatta Dhar N, et al. The template of the primary lymphatic landing sites of the prostate should be revisited: Results of a multimodality mapping study. *Eur Urol* 2008;53:118-125.
27. Mottet N, Bellmunt J, Bolla M, et al. EAU-ESTRO-SIOG guidelines on prostate cancer. Part 1: Screening, diagnosis, and local treatment with curative intent. *Eur Urol* 2017;71:618-629.
28. de Korne CM, Wit EM, de Jong J, et al. Anatomical localization of radiocolloid tracer deposition affects outcome of sentinel node procedures in prostate cancer. *Eur J Nucl Med Mol Imaging* 2019;46:2558-2568.
29. Harke NN, Godes M, Wagner C, et al. Fluorescence-supported lymphography and extended pelvic lymph node dissection in robot-assisted radical prostatectomy: A prospective, randomized trial. *World J Urol* 2018;36:1817-1823.
30. Nguyen DP, Huber PM, Metzger TA, Genitsch V, Schudel HH, Thalmann GN. A specific mapping study using fluorescence sentinel lymph node detection in patients with intermediate- and high-risk prostate cancer undergoing extended pelvic lymph node dissection. *Eur Urol* 2016;70:734-737.
31. Winter A, Kowald T, Paulo TS, et al. Magnetic resonance sentinel lymph node imaging and magnetometer-guided intraoperative detection in prostate cancer using superparamagnetic iron oxide nanoparticles. *Int J Nanomedicine* 2018;13:6689-6698.
32. De Bruycker A, De Bleser E, Decaestecker K, et al. Nodal oligorecurrent prostate cancer: anatomic pattern of possible treatment failure in relation to elective surgical and radiotherapy treatment templates. *Eur Urol* 2019;75:826-833.
33. Parker WP, Evans JD, Stish BJ, et al. Patterns of recurrence after postprostatectomy fossa radiation therapy identified by C-11 choline positron emission tomography/computed tomography. *Int J Radiat Oncol Biol Phys* 2017;97:526-535.
34. Schiller K, Sauter K, Dewes S, et al. Patterns of failure after radical prostatectomy in prostate cancer: Implications for radiation therapy planning after ^{68}Ga -PSMA-PET imaging. *Eur J Nucl Med Mol Imaging* 2017;44:1656-1662.
35. Calais J, Kishan AU, Cao M, et al. Potential impact of ^{68}Ga -PSMA-11 PET/CT on the planning of definitive radiation therapy for prostate cancer. *J Nucl Med* 2018;59:1714-1721.
36. Hahl G, Sauter K, Schiller K, et al. ^{68}Ga -PSMA-PET for radiation treatment planning in prostate cancer recurrences after surgery: Individualized medicine or new standard in salvage treatment. *Prostate* 2017;77:920-927.
37. Byrne K, Eade T, Kneebone A, et al. Delineating sites of failure following post-prostatectomy radiation treatment using ^{68}Ga -PSMA-PET. *Radiother Oncol* 2018;126:244-248.
38. Sinha S, Witzum A, Vasudevan H, et al. ^{68}Ga -PSMA-11 PET-based prostate cancer lymph node atlas reveals patterns of potential geographic miss in consensus pelvic nodal contours. *Int J Radiat Oncol Biol Phys* 2019;105:S136.
39. Schiller K, Stöhrer L, Düsberg M, et al. PSMA-PET/CT-based lymph node atlas for prostate cancer patients recurring after primary treatment: Clinical implications for salvage radiation therapy [e-pub ahead of print]. *Eur Urol Oncol*. <https://doi.org/10.1016/j.euo.2020.04.004>. Accessed May 23, 2020.
40. Delpon G, Escande A, Ruef T, et al. Comparison of automated atlas-based segmentation software for postoperative prostate cancer radiotherapy. *Front Oncol* 2016;6:178.
41. Jethwa KR, Hellekson CD, Evans JD, et al. ^{11}C -Choline PET guided salvage radiation therapy for isolated pelvic and paraortic nodal recurrence of prostate cancer after radical prostatectomy: Rationale and early genitourinary or gastrointestinal toxicities. *Adv Radiat Oncol* 2019;4:659-667.